1st Proceeding of International Conference on Science and Technology UISU (ICST)
"Contribution of Engineering Disciplines to Achieving Sustainable Development Goals Research Realizing the Vision of Golden Indonesia 2045"
ISSN: 3063-7929 (Online)
DOI: https://doi.org/10.30743/icst

Stability and Matching Techniques on Microwave Amplifier using Inhomogeneous Dielectric Resonator: Preliminary Study

Rashidah Che Yob[1)], Norizan Mohamed Nawawi[2)], Nur Hidayah Ramli[3)], Liyana Zahid[4)]
Faculty of Electronic Engineering & Technology (FKTEN), Department of Electronic, Universiti Malaysia Perlis (UniMAP), 02600 Pauh Putra, Perlis
rashidahcheyob@unimap.edu.my[1], norizan@unimap.edu.my[2], hidayahramli@unimap.edu.my[3], *and* liyanazahid@unimap.edu.my[4]

Abstract - Stability and matching techniques on microwave amplifier have been an important consideration to maintain the required performances, such as high power for the high-power amplifier and low noise for low noise amplifier. Simultaneously, the issues of the stability need more attention to avoid the presence of the oscillations. Typically, the stability factor and matching components of the microwave amplifier are frequency dependent. Thus, a frequency tunable mechanism is required to ascertain that frequency of the microwave amplifier resides within the stable region. The dielectric resonator is incorporated as the frequency tunable mechanism that implemented to overcome this issue. The characteristics of the dielectric resonator are evaluated on their physical parameter and material with different topologies of the parallel microstrip lines. This includes the spacing and curves configuration and the orientation of angular position for the dielectric resonator, especially for the multi-permittivity dielectric resonator. Regarding the preliminary study, the angular position of the multi-permittivity dielectric resonator does not influence the stability performances of microwaves amplifier, especially on the resonant frequency. The obtained best configuration of proposed dielectric resonator is consisting of 155-degree curves configuration with 19 mm spacing between the parallel microstrip lines for same waveguide port position. This configuration of the proposed dielectric resonator is incorporated as stability element and matching components that known as dielectric matching for conditional stable and unconditional stable transistors at 5 GHz.
Keywords Stability; Matching Techniques; Dielectric Matching; Transistor; Microwave Amplifier; Dielectric Resonator

1. INTRODUCTION

Generally, the stability and matching technique of the microwave amplifier is some optimum solutions, where it depends on the circuits requirements, such as the simplicity in practical realization, the frequency bandwidth, minimum noise figure, design implementation and adjustability, stable operations conditions, linearity, and sufficient harmonic suppression. Thus, many types of stability and matching networks are available [1-4], which including lumped element [5], transmission lines [6], and tunable matching network [7-9]. The qualitative summary of the stability and matching techniques for microwave amplifier of the previous research done are listed and summarized in Table 1.

Table 1: The qualitative summary of the stability and matching techniques for microwaves amplifier

Stability & matching networks		Freq. (GHz)	Amplifier Topologies	Issues	Performances	Ref.
Input	***Output***					
-	Tuneable impedance matching network (coupled inductors)	0.2-0.3	PA	• Efficiency • Maximum power output.	• Useful option for CMOS design when low-*Q* inductors must be used.	[8]
Narrowband tunable impedance-matching network (π-structure with varactors in series with inductors)		1	LNA	• Noise figure (NF). • Tunable matching network.	• Tuned in a 50% BW. • S_{11}=< -20 dB • S_{21}= > -3 dB	[9]
Lumped elements (L-shape network: Inductors & Capacitors)		4-8	LNA	• Gain. • NF.	• S_{11}= -50 dB • S_{21}= 13 dB • S_{12}=-15 dB • S_{22}=- 40 dB • *NF*= 2.2 dB • *VSWR*=1.5 • *K=1.07*	[10]
Load line matching.		2.5	PA	• Linearity. • Efficiency.	• Maximum efficiency power is 66%.	[11]
Combination L-L matching		1-10	LNA	• Gain.	• S_{21}= 10 dB	[12]

ISSN: 3063-7929 (Online)
DOI: https://doi.org/10.30743/icst

circuits.			• Stability factor. • NF.	• S_{12}=-49.59 dB • *NF*= 0 dB	
Feedback resistor for improved stability of the circuit (R = 500Ω). Lumped, distributed and radial stub elements for matching.	10	LNA	• Minimum NF. • High gain.	• S_{11}= -17.35 dB • S_{21}= 14.77 dB • S_{12}=-18 dB • S_{22}=-10.24 dB • *NF*= -0.775 dB	[13]
Lumped, distributed & radial stub elements.	10-15	LNA	• High gain. • Minimum NF.	• S_{11}= -17.15 dB • S_{21}= 14.35 dB • S_{12}=-17.023 dB • S_{22}=-16.92 dB • *NF*= -0.92 dB	[14]
Adaptive (automatic) impedance-matching network (capacitor-matrix)	1.3	PA	• Resonant frequency. • Power transfer efficiency.	• Power transfer efficiency increased up 88% when distances changes 0 to 1.2 m.	[15]
RLC feedback for stabilization. T and L matching network.	6	LNA	• NF. • Gain. • Stability factor.	• S_{11}= -17.2 dB • S_{21}= 14.14 dB • S_{12}=-23.5 dB • S_{22}=-6.29 dB • *NF*= 1.816 dB • *K=1.304*	[16]
Negative feedback circuit for stabilization. Smith Chart and tuning matching.	2.45	LNA	• Improved sensitivity of the systems. • Maximum gain.	• S_{11} & S_{22} = < - 15 dB • S_{21}= > 15 dB • *NF*= < 0.8 dB	[17]
- Two variable capacitors	2.14	PA	• Maximum PAE.	• PAE increased by 21.8 % from 33.4% to 55.2 %.	[18]
Smith chart utility	8	LNA	• Gain. • Stability analysis.	• *Gain*=10dB	[19]
Symbolic approach (Heuristic algorithm)-generated design variables values in-terms of these unknowns.	1-3	LNA	• Output power – *maintain the efficiency power at the same maximum level.* • Quality factor, *Q*. • Enhance efficiency.	• S_{11} & S_{22} =< -10 dB • S_{21}= > 10 dB • *NF*= < 1 dB	[20]
Distributed circuits elements (lumped elements matching & numerical optimization techniques)	1-2	PA	• Broadband matching.	• S_{11} =< -20 dB	[21]
RC feedback network (R=120 Ω, C=1pF)	4	PA	• Global stability analysis. • Effect of stabilization network. • Potential unstable PA.	• Efficient determination of the unstable operation conditions of microwave amplifiers.	[22]

ISSN: 3063-7929 (Online)
DOI: https://doi.org/10.30743/icst

PA: Power Amplifier; LNA: Low Noise Amplifier

Based on related works summarized in Table 1, the most issues are about gain, stability and noise factor. However, if the stability issues are not solved, gain and noise factor will be significantly affected. As mentioned previously, the stability factor is influenced by the changes in operating frequency. Some amplifiers can reside in either a stable or unstable region depending on the operating frequency. External disturbances such as temperature variation can only vary the frequency, thus making the amplifier susceptible to uncertainty in the aspect of stability. Therefore, the operating frequency needs to be easily controlled for such cases.

The work in [23] explores the use of cylindrical dielectric resonator (CDR) as frequency tunable elements. The placement of dielectric resonator with a constant physical parameter can tune the operating frequency of the two-way power divider; improving its performances for multifrequency operation without changing its physical dimensions. The advantages of DR is having high *Q*-factor, high radiation efficiency and also ease of the electromagnetic coupling made the DR is used to alter the properties of a normal power divider. This DR is provided dielectric loading to the T junction of the divider and also magnetically coupled with the microstrip lines of this power divider. By using the full-wave electromagnetic analysis of the divider structures, the implementation of such DR gives the input return loss better than 20 dB in operation of the divider at multiple frequencies.

The microstrip line configuration is also another important consideration that would influence the performance of the microwave circuits. The ideas to investigate the microstrip line configuration which is adopted by [24-25]. This microstrip line configuration is represented as coupling configuration between DR and monolithic microwave integrated circuits (MMICs) in [25] as the new developments that purposely to improve the phase noise [25] and high output power [24] of the dielectric resonator oscillator (DRO). In this article, this microstrip line configuration is investigated to explore the frequency changes of the microwave amplifier where should be operated at 5 GHz. Meanwhile, the uses of the dielectric resonator (DR) as frequency tunable elements gives great ideas to implement on microwave amplifier in order to ascertain the frequency of amplifier resides within the stable region. The characteristic of the DR is initially investigated through the multi-permittivity dielectric resonator (MPCDR) or also known an inhomogeneous DR. It is attracted attention to be explored due to their dual purpose can be served at one time. As earlier research presented regarding DR is usually using a homogenous DR that can serve only one purpose at one time. The uses of the multi-permittivity DR as in [26-28] have overcome the drawbacks of the homogenous DR, while the basic geometry of the resonator is maintained. Thus, the available theoretical, numerical and experimental tools can be effectively applied to the proposed inhomogeneous DRs.

In [26-28], the MPDR are represented by high and low permittivity with 90° pie-shaped sectors of each permittivity materials that positioned in non-adjacent quadrants. The high permittivity, ε_{r_1} represents by magnesium titanium oxide doped with cobalt ($MgTiO_3$ + Co) of 15 and only $MgTiO_3$ of 15.72 in [26-27] and [28], respectively. The ε_{r_1} of DR materials has high *Q*-factors that stored more of electromagnetic energy inside and also helps in achieving a strong coupling to the feeding structure (coupling implementation). Meanwhile, the low permittivity, ε_{r_2} is presented by Roger substrate (RT6010) of 10.2 and ($CoTiO_3$) of 9.85 in [28]. The ε_{r_2} of DR materials has tendencya to be operated in wider bandwidth (BW). The combination of the high and low permittivity plays important role in achieving wideband operation with strong coupling coefficients. The strong coupling coefficients gives the maximum radiation pattern of the electric and magnetic fields. Besides that, the wider BW can handle high data rates, multi-lingual communication, multi-communication channels and control data traffic of the modern communication systems. By referring [28], the different single and multi-permittivity geometries of CDR are evaluated for wideband performances.

2. PRELIMINARY STUDY ON DIELECTRIC RESONATOR

The specification of the preliminary study on dielectric resonator (DR) includes the substrate and related parameter, parameter of dielectric resonator and microstrip line dimension and its characteristics are presented here. In addition, the preliminary studies on dielectric resonator are evaluated on their physical parameter and material with different topologies of the parallel microstrip lines. This involves the spacing and curves configuration and the orientation of angular position for the dielectric resonator, especially for the multi-permittivity dielectric resonator. The details about the specification and preliminary study of the physical parameter and material with different topologies of the parallel microstrip lines for dielectric resonator are discussed.

2.1 Dielectric Resonator Specification

2.1.1 Substrate RO4003C series and related parameters

The selection of the board material is very important to be used for high operating frequency implementation, which is the C-band frequency at 5 GHz. Hence, the RO4003C substrate is a product by Rogers Corporation has been chosen for this research. The RO4003C substrate has low dielectric tolerance and low loss. Furthermore, its excellent electrical performance makes it a good choice for applications at high operating frequencies range.

ISSN: 3063-7929 (Online)
DOI: https://doi.org/10.30743/icst

Moreover, it also offers a low cost for circuit fabrication. The electrical characteristics of the RO4003C material used in modeling dielectric resonator circuit are stated in Table 2 [29].

Table 2: Electrical characteristics of the RO4003C [29]

Parameters	Symbol	Dimension
Dielectric constant	ε_r	3.38 ± 0.05
Dissipation factor	tan δ	0.0027
Thermal coefficients of εr	°C	+40
Substrate thickness	H	0.813 mm
Copper thickness	T	0.035 mm
Conductor conductivity	σ	5.8 x 107 S/m

At the speed of light and the operating frequency of 5 GHz as well as the dielectric constant of 3.38 is calculated as follow:

$$\lambda_g = \frac{c}{\sqrt{\varepsilon_r} f} = \frac{3\times10^8}{\sqrt{3.38}(5G)} \quad (1)$$

$$\lambda_g = 32.63\ mm \quad (2)$$

$$\lambda_g/_2 = 16.31\ mm \quad (3)$$

$$\lambda_g/_4 = 8.15\ mm \quad (4)$$

Meanwhile, the dimensions of the substrate with the copper ground plane as shown in Fig. 1 is summarized in Table 3.

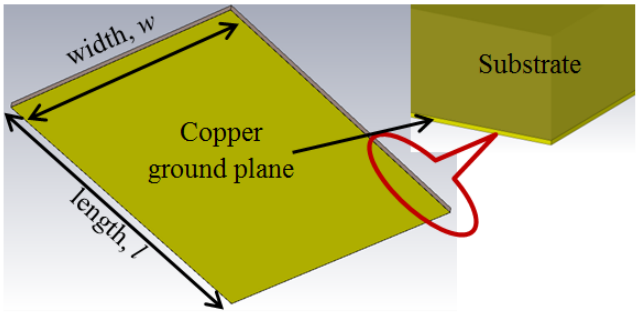

Figure. 1: Dimension of the substrate with the copper ground plane.

Table 3: The grounded substrate dimensions

Parameters	Value (mm)
Length, *l*	32.61
Width, *w*	30
Height of substrate, *h*	0.813
Thickness of copper, *t*	0.035
Substrate material	Duroid (Roger RO3004C)
Grounded material	Copper

2.1.2 Dielectric resonator configuration and characteristics

1st Proceeding of International Conference on Science and Technology UISU (ICST)
"Contribution of Engineering Disciplines to Achieving Sustainable Development Goals Research Realizing the Vision of Golden Indonesia 2045"
ISSN: 3063-7929 (Online)
DOI: https://doi.org/10.30743/icst

The structure of the dielectric resonator mainly consists of three basic layers; the bottom layer is copper, followed by the substrate that places dielectric resonator above it together with feeding mechanism, which the microstrip line. Lastly, the upper layer is filled up with the vacuum to avoid the field radiation in the air or block the noise and interferences as illustrated in Fig. 2 (a). Meanwhile, the front view of the parallel CDR is presented in Fig. 2 (b). The parametric analysis for the parallel CDR is investigated for same waveguide port position as in Fig. 2 (c).

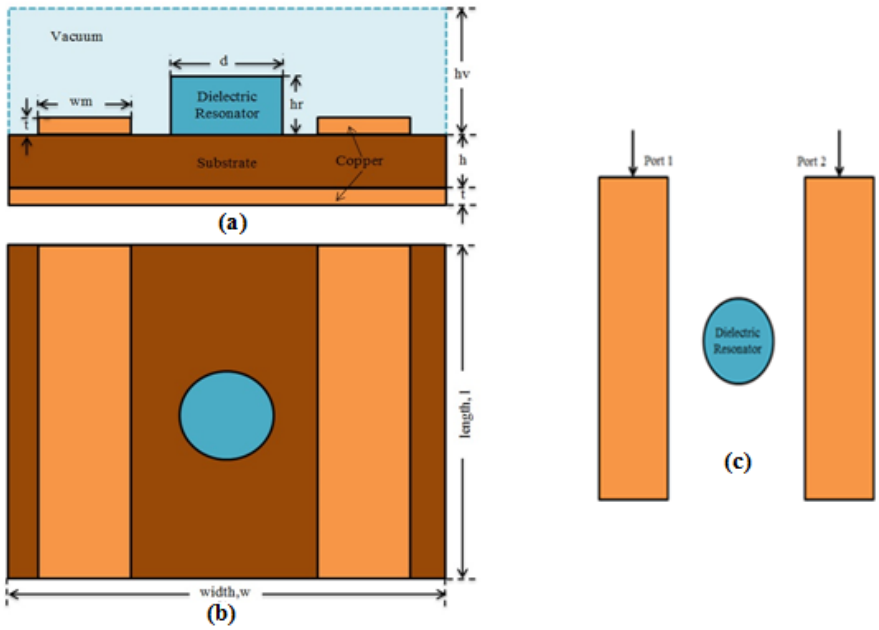

Figure. 2: Parallel cylindrical dielectric resonator: (a) Cross-sectional view, (b) front view and (c) same waveguide port position.

The common parameters of the dielectric resonator are referred from [26-28], especially their dielectric permittivity of the DR. The inhomogeneous CDR is formed by two different dielectric materials, which is Magnesium Titanate Oxide, ε_{r1} and Cobalt Titanate Oxide, ε_{r2} where also known $MgTiO_3$ (MTO) and $CoTiO_3$ (CTO), respectively. The value of this inhomogeneous CDR of each material is presented in Fig. 3 [28].

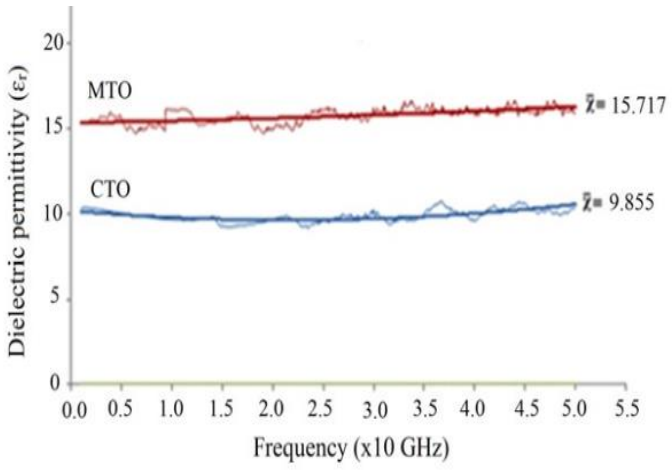

Figure. 3: The value of the dielectric permittivity of MTO and CTO for the inhomogeneous CDR [28].

The details parameters and characteristics of the inhomogeneous CDR are calculated using (5) for its diameters, which about 2% in the range of *a/b* [26, 30]. The details parameters and characteristics of the inhomogeneous CDR are summarized in Table 4.

$$f_{GHZ} = \frac{34}{a_{mm}\sqrt{\varepsilon_r}}\left(\frac{a}{L} + 3.45\right) \quad (5)$$

Table 4: Inhomegenous CDR parameters and characteristics [28]

ISSN: 3063-7929 (Online)
DOI: https://doi.org/10.30743/icst

Property	Dielectric Permittivity		Loss Tangent		Parameters	
	MTO (ε_{r1})	*CTO* (ε_{r2})	*MTO* (*tan δ*)	*CTO* (*tan δ*)	*Thickness*	*Radius*
Value	15.72	9.86	-0.0133	-0.0143	2.5 mm	7.5 mm

Both MTO and CTO also reported in [31] claims this material is well known as low loss dielectric ceramics and have wide applications in communications systems, especially as base materials to elaborate the resonators, filters, antennas, radar and global positioning systems that operating at microwaves frequencies.

2.1.3 Microstrip line dimensions and characteristics

In this article, the microstrip line is used as the feeding mechanism for the dielectric resonator. The parallel microstrip lines produce the optimum power level with more stability that will be fulfilled the purpose of the dielectric resonator as stability elements and matching components in this work. The dimension of the parallel microstrip lines would be obtained by using (6) until (9) depending on the width to the height ratio (Javier, 2017; Pozar, 2005).

For $\frac{w}{h} < 1$,

$$\varepsilon_{eff} = \frac{\varepsilon_r+1}{2} + \frac{\varepsilon_r-1}{2}\left[\left(1+\frac{12h}{w}\right)^{-0.5} + 0.04\left(1-\frac{w}{h}\right)^2\right] \quad (6)$$

$$Z_o = \frac{60}{\sqrt{\varepsilon_{eff}}}\ln\left(\frac{8h}{w}+0.25\frac{w}{h}\right) \quad (7)$$

For $\frac{w}{h} > 1$,

$$\varepsilon_{eff} = \frac{\varepsilon_r+1}{2} + \frac{\varepsilon_r-1}{2}\left(1+\frac{12h}{w}\right)^{-0.5} \quad (8)$$

$$Z_o = \frac{377}{\sqrt{\varepsilon_{eff}}\left[\frac{w}{h}+1.393+\left(0.667ln\left(\frac{w}{h}+1.444\right)\right)\right]} \quad (9)$$

where *h* is the substrate thickness, *w* is the microstrip line width, *t* is the conductor thickness, ε_{eff} is an effective dielectric constant of the substrate, and ε_r is a dielectric constant of the substrate.

In this article, the dimension of parallel microstrip lines is calculated using *impedance calculation* option in CST software, where *h* is the height of substrates, *eps* is the Epsilon (permittivity) of the substrates and *w* is the width of the microstrip line to yield 50 Ω line as in Fig. 4.

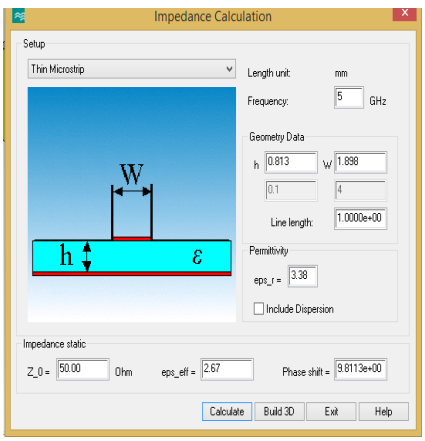

Figure 4: Impedance calculator tools for microstrip line in CST software.

ISSN: 3063-7929 (Online)
DOI: https://doi.org/10.30743/icst

The length of the parallel microstrip lines is kept *λ/2*, to keep the overall size of the substrate. The dimension and material of the parallel microstrip lines are summarized in Table 5. Practically, the waveguide port is realized by an SMA connector for providing connectivity for the assemblies within the equipment where the required coaxial connections.

Table 5: The dimensions and material of the parallel microstrip lines

Parameters	Value (mm)
Length, *l*	λ
Width, *w*	1.898
Thickness of microstrip line, *t*	0.035
Microstrip line material	Copper

3. PRELIMINARY STUDY ON DIELECTRIC RESONATOR

The preliminary studies on dielectric resonator are investigated for spacing and curve configuration of the parallel microstrip lines and angular position of the CDR, especially for inhomogeneous CDR. The objectives of the preliminary studies that also knowns as the parametric study on dielectric resonator to identify the influences involved in any changes and to determine the best configuration of the parallel CDR. The details of the parametric study are discussed in the next following subsection.

3.1 Parallel Microstrip Lines Spacing

Firstly, the parametric study focuses on the different spacing or known as the coupling coefficients as shown in Fig. 5. The suitable distance of spacing is needed to determine between parallel microstrip lines and the CDR.

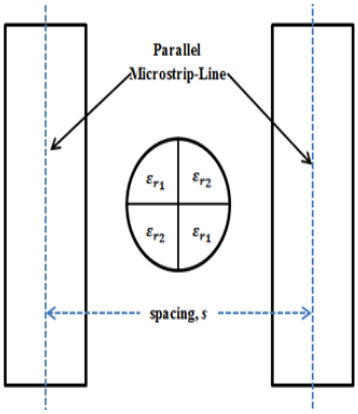

Figure 5: The configuration for the spacing of parallel microstrip lines.

Seven different spacing between parallel microstrip lines and the CDR is examined for 10, 13, 15, 17, 19, 21 and 25 (mm) as in Fig. 6. The coupling distances of 15 mm between the parallel microstrip lines and the CDR is taken as the references based on the half-width of the overall dimensions of the DR. Then, the distances between the coupling coefficients are analyzed by adding and subtracting the spacing distances between parallel microstrip lines. Then, the findings for this investigation are presented as in Fig. 7 and then summarized in Table 6.

1st Proceeding of International Conference on Science and Technology UISU (ICST)
"Contribution of Engineering Disciplines to Achieving Sustainable Development Goals Research Realizing the Vision of Golden Indonesia 2045"
ISSN: 3063-7929 (Online)
DOI: https://doi.org/10.30743/icst

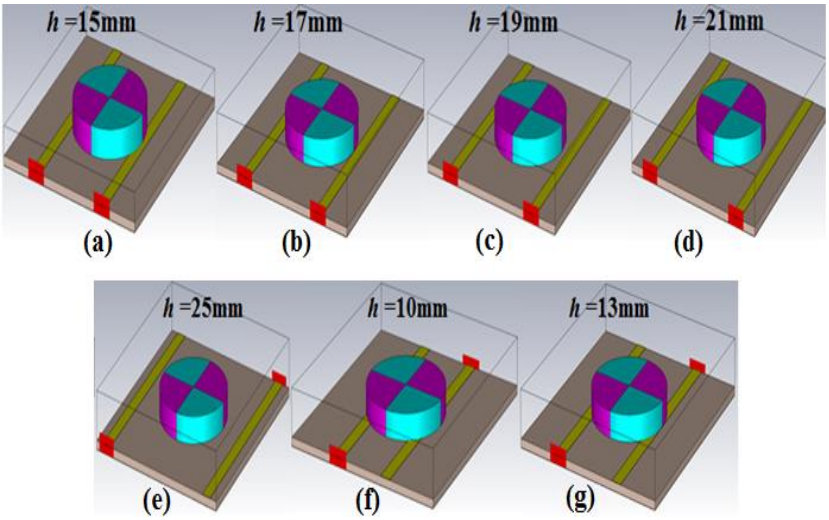

Figure 1: The different spacing (coupling coefficients) between the parallel microstrip lines and the CDR: (a) 15, (b) 17, (c) 19, (d) 21, (e) 25, (f) 10 and (g) 13 mm.

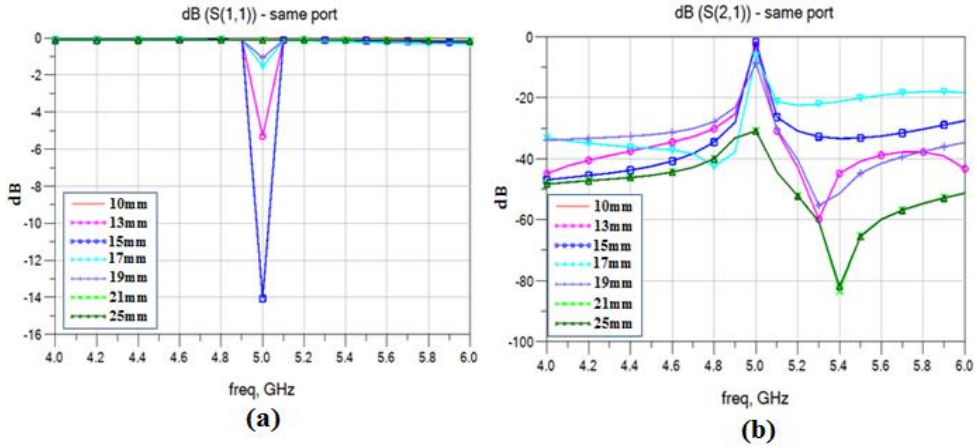

Figure 7: The obtained *S*-parameters for different spacing between parallel microstrip lines and the CDR: (a) S_{11} and (b) S_{21} responses.

Table 6: Different spacing between the CDR and parallel microstrip lines

Coupling Distance (mm)	SAME PORT		
	Freq (GHz)	***S_{11} (dB)***	***S_{21} (dB)***
10	4.994	-4.257	-2.924
13	4.998	-8.408	-1.809
15	5.000	-12.829	-1.436
17	4.998	-18.091	-1.309
19	4.984	-18.710	-1.516
21	4.972	-13.297	-2.019
25	4.954	-6.935	-5.133

The obtained *S*-parameters responses (S_{11} and S_{21}) for different spacing between parallel microstrip lines and the CDR, the best performances are at 17 and 19 (mm) of the coupling spacing. The obtain return loss is around -18 dB, which has a good agreement with the expected theoretically. However, their operating frequency is not accurately operated at 5 GHz. The obtained results show when the coupling spacing is too far or too close between the inhomogeneous CDR and a parallel microstrip line, the return loss responses is less than 10 dB. The suitable distance needs to be identified between the CDR and a parallel microstrip lines. The next preliminary study of the curves configuration of parallel microstrip lines is only considered the spacing distance of 17 and 19 (mm) between the CDR and parallel microstrip lines.

ISSN: 3063-7929 (Online)
DOI: https://doi.org/10.30743/icst

3.2 Parallel Microstrip Lines Curves Configuration

The next parametric study of the parallel microstrip lines is curved configuration at λ/4 of the wavelength, which are aims to investigate the effect of curves configuration on the return loss and insertion loss. The different curves configuration at λ/4 of the wavelength is evaluated for 65°, 90°, 155°, and 165° as represented in Fig. 8 below.

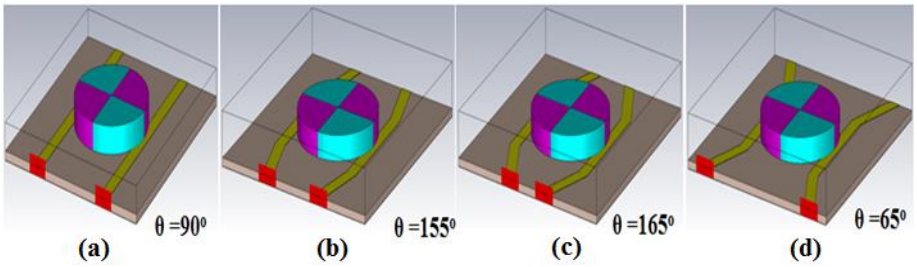

Figure 8: The different curve configuration at λ/4 of the wavelength for parallel microstrip lines: (a) 90°, (b) 155°, (c) 165° and (d) 65°.

The most common configuration of 90° curve configuration is used as references like mentioned in [32]. The different curve configuration is changed in order to analyze the best performance of the parallel microstrip lines. The obtained results for this parametric study are illustrated in Fig. 9 and stated in Table 7. This parametric study shows the best results are represented by the curve configuration of 90° and 155°. However, only the curve response of 155° with 19 mm of coupling spacing is shown accurately at 5 GHz of resonant frequency. Therefore, the parallel microstrip line which offers the best performance and can operate at 5 GHz is with 19 mm of coupling space and 155° of curves configuration. Thus, this best configuration will be used in the next investigation for the orientation of the angular position for proposed inhomogeneous CDR.

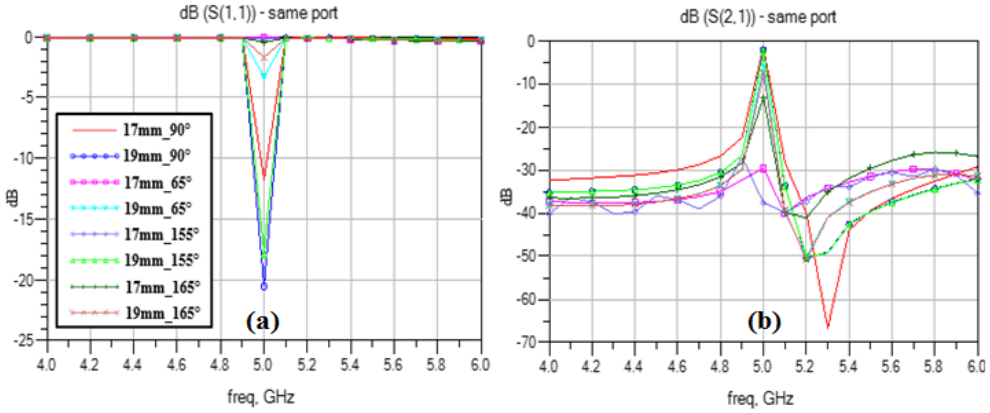

Figure 9: The obtained *S*-parameter of (a) S_{11} and (b) S_{21} responses for the different curved configurations at a λ/4 wavelength for parallel microstrip lines.

Table 7: Different curved configurations at a λ/4 wavelength of a parallel microstrip lines

Curves Configuration	Different Curved Configurations					
	17 mm			19 mm		
	Freq (GHz)	S_{11} *(dB)*	S_{21} *(dB)*	*Freq (GHz)*	S_{11} *(dB)*	S_{21} *(dB)*
65°	4.982	-4.370	-35.391	5.592	-14.047	-27.980
90°	4.998	-18.091	-1.309	4.984	-18.710	-1.516
155°	5.012	-18.010	-1.721	5.000	-20.538	-2.180
165°	5.012	-13.382	-2.677	4.999	-9.018	-3.415

3.3 The Inhomogeneous Cylindrical Dielectric Resonator Angular Position

This investigation is purposely to determine the best angular position that ensures the maximum electromagnetic coupling from the feeding structure to the resonator. The different angular position of the inhomogeneous CDR is evaluated, which are 0°, 10°, 27.5°, 30°, and 55° as in Fig. 10. The orientation of angular position initially refers to the longitudinal axis of the parallel microstrip line as the references. Then, the different values for the orientation of angular position are changed or rotated in an anticlockwise direction.

ISSN: 3063-7929 (Online)
DOI: https://doi.org/10.30743/icst

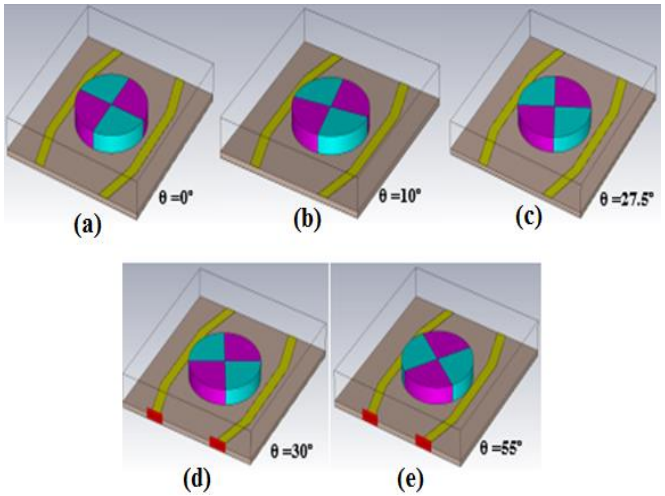

Figure 10: The different orientation of angular position for the inhomogeneous CDR: (a) 0°, (b) 10°, (c) 27.5°, (d) 30° and (e) 55°.

The findings of the *S*-parameters (S_{11} and S_{21}) responses for this preliminary study are shown in Fig. 11 and summarized in Table 8.

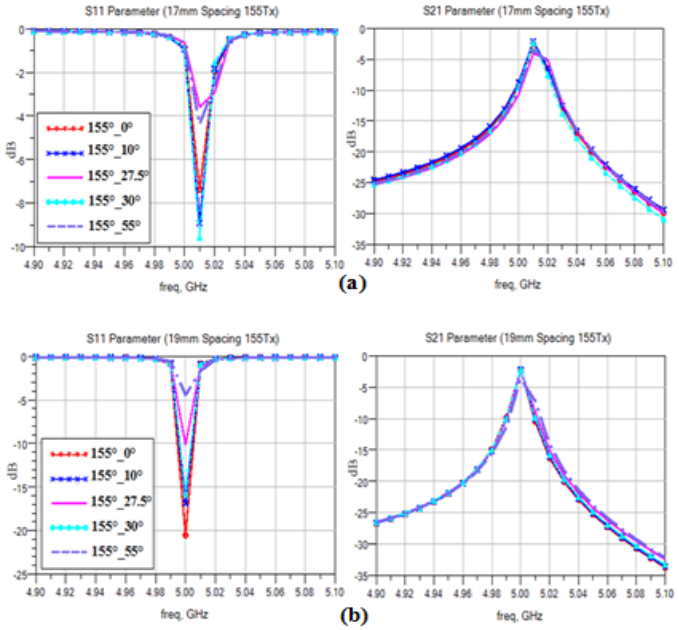

Figure 11: Different orientation of the angular position for the proposed inhomogeneous CDR of 155° curved configuration at a λ/4 wavelength with (a) 17 and (b) 19 (mm) of coupling spacing.

Table 8: Different orientation of the angular position for inhomogeneous CDR with different spacing of 17 and 19 (mm) for 155° curved configuration

Angular Position	Curved Configuration (155°)					
	Distance Coupling (17mm)			Distance Coupling (19mm)		
	Freq (GHz)	*S_{11} (dB)*	*S_{21} (dB)*	*Freq (GHz)*	*S_{11} (dB)*	*S_{21} (dB)*
0°	5.012	-18.010	-1.721	5.000	-20.538	-2.180
10°	5.012	-21.250	-1.569	5.000	-16.860	-2.206
27.5°	5.014	-15.573	-1.759	5.002	-14.228	-2.110
30°	5.012	-27.539	-1.852	5.000	-15.765	-2.142
55°	5.014	-17.195	-1.663	5.004	-12.251	-2.120

The obtained S_{11} and S_{21} responses in Table 8 show the best performance which operates more closely to the resonant frequency of 5 GHz is 19 mm of coupling spacing with 155° of curved configuration. The angular position of the inhomogeneous CDR did not really affect their resonant frequency. The optimum performances obtained

ISSN: 3063-7929 (Online)
DOI: https://doi.org/10.30743/icst

without the angular position, which 20.538 dB of S_{11} and 2.180 dB of S_{21}. Thus, the homogenous CDR are considered in the implementation for stability performances on microwave amplifier. It can be concluded, the best configuration of the CDR consists of 155° curved configuration with 19 mm of spacing will be used as a dielectric matching component on microwave amplifier.

4. CONCLUSIONS

This article presents the stability and matching techniques on microwave amplifier by implementation dielectric resonator as dielectric matching for conditionally stable and unconditionally stable transistors at 5 GHz. All the parameters of the preliminary studies are based on the common and empirical investigation. For the preliminary study on microwave amplifier, the characteristics of dielectric resonator, especially for the inhomogeneous CDR are referred from [27], but the difference of the feeding mechanism is used. In this article, the parallel microstrip lines at 5 GHz resonant frequency is uses as the feeding mechanism for the dielectric resonator. In addition, the investigation in [27] to optimize the antenna sector size and permittivity operated in wider bandwidth (BW) with strong electromagnetic coupling. Meanwhile, the parametric studies in this article are focused on coupling coefficients and curved configuration between parallel microstrip lines and the CDR which affected the resonant frequency for microwave applications, such as an oscillator, amplifier, and filter. The parametric analysis of the parallel CDR is analyzed based on *S*-parameters for different coupling coefficients. Then, the next investigation involving curve configuration is focused on acquiring optimum performance at 5 GHz examined by different curve configuration at the $\lambda/4$ wavelength of the parallel microstrip line. This parametric study indicates the best performance of S_{11} and S_{21} of 5 GHz occurs at 19 mm spacing distance with 155 degrees of curved configuration is 20.538 dB and 2.142 dB, respectively. This curve position configuration improves the performance of parallel inhomogeneous CDR by 9.77% from the performance of spacing coupling and shifted resonant frequency to 5 GHz. Then, the orientation of the angular position is analyzed, especially for inhomogeneous CDR. The obtained results show the optimum performance at 5 GHz is without the angular position which indicates the orientation of the angular position can be ignored. Regarding to the preliminary study, the obtained best configuration of proposed dielectric resonator is 155˚ curves configuration with 19 mm spacing between the parallel microstrip lines for same waveguide port position.

ACKNOWLEDGEMENTS

The authors thanks to Universiti Malaysia Perlis (UniMAP) for the funding and support of the research work under Research Materials Fund (RESMATE), 9001-00627. The members of Faculty of Electronic Engineering Technology, UniMAP are also specially thanks for their helps and kindness.

REFERENCES

[1]. Eroglu, A. 2010. Stabilization of Class E amplifiers with a diode network. AEU - International Journal of Electronics and Communications, 64(3), 224–230.

[2]. Han, Y., & Perreault, D. J. 2006. Analysis and design of high efficiency matching networks. IEEE Transactions on Power Electronics, 21(5), 1484–1491.

[3]. Grebennikov, A. 2005. RF and microwave power amplifier design. New York: McGraw-Hill Professional Engineering.

[4]. Pozar, D. M. 2005. Microwave engineering. 3rd Edition. New York: Wiley.

[5]. Lin, Y.-S., Wang, C.-C., & Lee, J.-H. 2014. Design and implementation of a 1.9-22.5 GHz CMOS wideband LNA with dual-RLC-branch wideband input and output matching networks. Microwave and Optical Technology Letters, 56(3), 677–684.

[6]. Vimal, S. & Maheshwari, M. 2016. Design and performance improvement of a low noise amplifier with different matching techniques and stability network.International Journal of Engineering Research & Science (IJOER), 2(3), 1-10.

[7]. Alimenti, F., Virili, M., Mezzanotte, P., Roselli, L., Rericha, V., Pokorny, M., Iorio, F., Gaddi, R. & Schepens, C. 2014. A RF-MEMS based tuneable matching network for 2.45 GHz discrete-resizing CMOS power amplifiers.Radioengineering, 23(1), 328-337.

[8]. Fabbro, P. A. D. & Kayal, M. 2008. RF power amplifier employing a frequency tunable impedance matching network based on coupled inductors. ElectronicLetters, 44(19), 1131 -1132.

[9]. Hoarau, C., Corrao, N., Arnould, J.-D., Ferrari, P., & Xavier, P. 2008. Complete design and measurement methodology for a tunable RF impedance-matching network. IEEE Transactions on Microwave Theory and Techniques, 56(11), 2620–2627.

ISSN: 3063-7929 (Online)
DOI: https://doi.org/10.30743/icst

[10]. Iyer, M., & Shanmuganantham, T. 2017. Design of LNA for C band applications, in: IEEE International Conference on Circuits and Systems (ICCS), Thiruvananthapuram, India, 211-214.

[11]. Veeranjaneyulu, M. & Anuradha, B. 2016. Design & simulation of radio frequency power amplifiers for high efficiency and without affecting linearity. International Journal on Recent and Innovation Trends in Computing and Communication, 4(8), 46-49.

[12]. Madhura, P. J. & Savita, B. B. 2015. Efficient designing techniques for low noise amplifier, in: 22nd IRF International Conference, Pune, India, 106-108.

[13]. Fallahnejad, M. & Alireza, K. 2014. Design of low noise amplifiers at 10 GHz and 15 GHz for wireless communications systems. IOSR Journal of Electrical and Electronic Engineering (IOSR-JEEE), 9(5), 47-53.

[14]. Fallahnejad, M., Yasaman, N. & Alireza, K. 2015. Design and simulation of low noise amplifier at 10 GHz by using GaAs High Electron Mobility transistor. IOSR Journal of Electrical and Electronic Engineering (IOSR-JEEE), 10(5), 29-34.

[15]. Lim, Y., Tang, H., Lim, S. & Park, J. 2014. An adaptive impedance-matching network based on a novel capacitor matrix for wireless power transfer. IEEE Transactions on Power Electronics, 29(8), 4403-4413.

[16]. Senthilkumar, D., Uday, P. K. & Santosh, J. 2013. Design and comparison of different matching techniques for low noise amplifier circuit. International Journal Engineering Research and Applications (IJERA), 3(1), 403-408.

[17]. Yu-na, S. & Geng, L. 2012. Design of a low noise amplifier of RF communication receiver for mine, in IEEE Symposium on Electrical & Electronics Engineering (EEESYM), Kuala Lumpur, Malaysia, 125-127.

[18]. Gao, S. Wang, Z. & Chan-Wang, P. 2010. A novel RF tunable impedance matching network for correcting the tested result deviation from simulated result, in Proceedings of 2010 IEEE Asia-Pacific Conference on Applied Electromagnetics (APACE 2010), Port Dickson, Negeri Sembilan, Malaysia, 1 -4.

[19]. Fuzy, C. & Zolomy, A. 2010. Design of broadband complex impedance-matching networks and their applications for broadbanding microwave amplifiers, in: 18th International Conference on Microwave Radar and Wireless Communications (MIKON), Vilnius, Lithuania, 1-4.

[20]. Boughariou, M., Fakhfakh, M. & Loulou, M. 2010. Design and optimization of LNAs through the scattering parameters, in: 15th IEEE MediterraneanElectrotechnical Conference (MELECON), Valletta, Malta, 764-767.

[21]. Khah, S. K., Singh, P., Rabra, S., Saxena R. & Chakarvarty, T. 2007. Broadband impedance matching technique for microwave amplifiers, in: IEEE Applied Electromagnetics Conference (AEMC), Kolkata, India, 1-4.

[22]. Collado, A., Ramirez, F. & Suarez, A. 2004. Analysis and stabilization tools for microwave amplifiers. IEEE MTT-S Digest, 945-948.

[23]. Jain, A., Hannurkar, P. R., Pathak, S. K., Biswas, A. & Srivastva, M. 2014. Improved performance of two-way power divider using dielectric resonator. Microwave and Optical Technology Letters, 56(4), 858-861.

[24]. Su, Y., Zhao, H. L., Liu, X. F., & Huang, L. H. 2012. Design of the dielectric resonator oscillator with buffer amplifier. Advanced Materials Research, 433-440, 4536–4540.

[25]. Yan, G. 2008. The design of the Ku band dielectric resonator oscillator, in: International Conference on Electronic Packaging Technology & High Density Packaging (ICEPT-HDP), Shanghai, China, 1 -3.

[26]. Ullah, U. 2016. Study of inhomogeneous dielectric resonators for linearly/circularly polarized microwave antenna applications. PhD Thesis, Universiti Sains Malaysia, MALAYSIA.

[27]. Ullah, U., Ali, W. F. F. W., Ain, M. F., Mahyuddin, N. M. & Ahmad, Z. A. 2015. Design of a novel dielectric resonator antenna using MgTiO3-CaTiO3 for wideband applications. Materials and Design, 85, 396-403.

[28]. Ullah, U., Ain, M. F., Othman, M., Zubir, I., Mahyuddin, N. M., Ahmad, Z. A. & Abdullah, M. Z. 2014. A novel multi-permittivity cylindrical dielectric resonator antenna for wideband applications. Radioengineering, 23, 1071-1076.

[29]. Rogers Cooperation. 2011. RO4000 Series High Frequency Circuit Materials, Advanced Connectivity Solutions, Available https://www.rogerscorp.com/documents/726/acm/RO4000-Laminates---Datasheet.pdf.

[30]. Mahyuddin, N. M. 2006. Design and implementation of a 10 GHz dielectric resonator oscillator. Master Thesis, Universiti Sains Malaysia, MALAYSIA.

[31]. Marulanda, J. I., Lina. R. A. A., Carvalho, M. C. R., Almeida, A. F. L., Sombra, A. B. S. & Demenicis, L. S. 2009. Characterization of dielectric properties of screen-printed MgTiO3-CaTiO3 composite thick films in the microwave frequency range, in: IEEE MTT-S International Microwave and Optoelectronics Conference (IMOC), Belem, Brazil, 211 -214.

ISSN: 3063-7929 (Online)
DOI: https://doi.org/10.30743/icst

[32]. Mahyuddin, N. M., Ain, M. F., Hassan, S. I. S. & Singh, M. 2006. A 10 GHz PHEMT dielectric resonator oscillator, in: Proceedings of the IEEE International RF and Microwave Conference, Putrajaya, Malaysia, 26-30.

[33]. Hewlett-Packard. 1997. 2-18 GHz Ultra Low Noise Pseudomorphic HEMT (ATF-36077), Technical Data, Available www.hp.woodshot.com/hprfhelp/4_downld/products/xrs/atf36077.pdf.

[34]. Fujitsu Semiconductor. 1998. FLC053WG Datasheets: C-band Power GaAs FETs, Available https://www.datasheets360.com/pdf/7214091158553669565.